RSC Sustainability

ROYAL SOCIETY OF CHEMISTRY

COMMUNICATION

View Article Online
View Journal | View Issue



Cite this: *RSC Sustainability*, 2025, **3**, 5459

Received 5th September 2025
Accepted 10th October 2025

DOI: 10.1039/d5su00728c

rsc.li/rscsus



# Recovering spent lithium nickel manganese cobalt (NMC) oxide cathodes from Li ion batteries for use as oxygen evolution reaction electrocatalysts

Arshdeep Kaur,[ab] Hongxia Wang,[ab] Michael R. Horn,[c] Jessica Crawford[ac] and Anthony P. O'Mullane *[abd]

Li ion battery (LIB) waste is an emerging environmental issue. Here we show that a typical LIB cathode material such as nickel manganese cobalt (NMC) oxide can be recovered and used directly as an electrocatalyst for the oxygen evolution reaction (OER). However, the impact of battery history indicates some decrease in OER performance.

## Sustainability spotlight

As the adoption of lithium ion batteries in many sectors accelerates, the challenge of battery waste is rapidly emerging. This research demonstrates an innovative circular economy approach by directly repurposing spent nickel manganese cobalt (NMC) cathode materials as electrocatalysts for the oxygen evolution reaction which is a critical process in water splitting technology. The study reveals that while extensive battery cycling (up to 200 cycles) impacts electrocatalytic performance due to particle pulverization and surface chemistry changes, the recovered materials still maintain substantial activity for renewable energy applications. Importantly, this direct recycling pathway is particularly promising for treating battery manufacturing waste where *ca.* 7% of batteries fail quality assurance during production. By eliminating costly multiple chemical leaching processes and creating immediate value from battery waste, this approach transforms what would be an environmental liability into functional materials for clean energy technologies. This work demonstrates how sustainable materials science can address multiple environmental challenges simultaneously, turning a growing battery waste stream into a resource for advancing renewable energy technology.

## Introduction

Lithium-ion batteries (LIBs) are used in various applications such as electric vehicles, grid level storage, and portable electronics.[1] In most commercial LIBs, graphite serves as the standard material for the anode,[2] implying the cathode material is a key factor in determining the battery's energy density and operating voltage. Nickel-rich layered oxides, such as $LiNi_xCo_y$ $Al_zO_2$ and $LiNi_xCo_xMn_zO_2$, as well as nickel-rich cobalt-free oxides, are prominent transition metal oxides that are often used in LIBs.[3] At any stage of their lifecycle, the presence of flammable and toxic substances in LIBs means that improper disposal can lead to significant environmental and safety concerns.

Therefore, recycling LIBs has gained significant attention not only because of environmental concerns but also resource limitations and our ever-increasing energy demands for storing renewable electricity and powering modern technologies. With increasing electrification of industry and transport there will be a significant level of battery waste to deal with in the coming decades that can be viewed as a resource rather than a waste product. This concept of urban mining is gaining traction as a means of alleviating this upcoming problem. In fact the global recycled battery market is expected to reach $23.72 billion by 2030,[4] and the number of recycling companies focused on LIBs is increasing in Europe, North America, and Asia.[5] However, of more immediate concern is the amount of battery scrap generated during the manufacturing process which consists of defective cells that do not meet quality assurance standards. The estimated global average scrap rate was 7.67% for 2023[6] while it has also been predicted that production scrap will account for more than half of the total LIB recycling source until 2025.[7] The recycling of LIB materials typically involves either physical recovery techniques or costly chemical recycling methods.[8,9] To minimize cost and maximize the utilization of transition metals in LIB cathode materials, work is underway on developing straightforward methods to directly use recycled LIB components[10] such as LCO (Lithium Cobalt Oxide) cathodes from spent LIBs as electrocatalysts for the oxygen evolution reaction (OER).[11] The direct use of recovered cathode materials alleviates chemical leaching processes which also generate a waste stream and therefore offers an alternative use of spent batteries or battery scraps discarded during production.

[a]*School of Chemistry and Physics, Queensland University of Technology (QUT), Brisbane, QLD 4001, Australia. E-mail: anthony.omullane@qut.edu.au*
[b]*Centre for Materials Science, Queensland University of Technology (QUT), Brisbane, QLD 4001, Australia*
[c]*Banyo Pilot Plant Precinct, Queensland University of Technology (QUT), Brisbane, QLD 4001, Australia*
[d]*QUT Energy Transition Centre, Queensland University of Technology (QUT), Brisbane, QLD 4001, Australia*

We have previously shown that NMC oxides with compositions of NMC 622 and NMC 811 that are typically used as LIB cathodes have inherently good electrocatalytic activity for the OER where NMC 622 with the lower Ni content has better activity than NMC 811.[12] However, it is not clear what impact battery cycling has on the OER performance of this material. Therefore, in this work we recover NMC 622 from batteries cycled up to 200 times at 1C and investigate the performance of the material for the OER in 1 M KOH electrolyte and determine the effect of battery history on direct recycling of NMC cathodes.

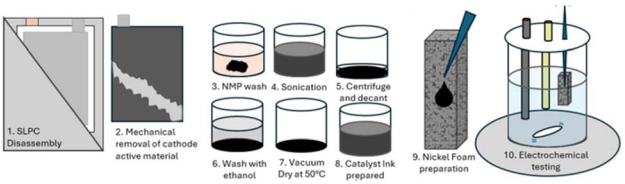


Scheme 1 Recovery process for isolating and testing NMC 622 for the OER.

## Experimental

### Materials

Potassium hydroxide (99.99%), absolute ethanol and nickel foam (NF) were purchased from Sigma Adrich. Milli-Q water with resistivity of 18.2 MΩ cm was used for the preparation of electrolyte solutions. The battery cell material was NMC 622, manufactured by Targray.

### Methodology of battery cell preparation

The slurry recipe for cathodes was 93% active material (AM), 4% carbon black (CB) and 3% PVDF. Graphite-based anodes were prepared in a similar way using commercially relevant binders. The cells constructed were of a small pouch cell design. The cells were tested on a Biologic BCS-810 workstation, operated by BT-Lab software. Details of the cell components and battery performance of the constructed cells are presented in Table 1.

### Cathode recovery

After the battery cells completed cycling, the electrode material was mechanically removed from the foil and placed in NMP (*N*-methyl-2-pyrrolidone) to remove the PVDF binder which in principle can be re-used. Then, sonication was performed for an hour in NMP. The material was then centrifuged after sonication to retrieve the powder and washed in ethanol and finally left to settle overnight. The top layer was decanted and then dried in a vacuum oven. This recovery process is illustrated in Scheme 1.

### Electrochemical experiments

A Biologic VSP workstation was used with a three-electrode cell configuration. A leakless Ag/AgCl (eDAQ Pty Ltd) and a high purity graphite rod (1 mm diameter, Johnson Matthey Ultra "F" purity grade) were used as the reference and counter electrodes, respectively. NF (1 × 1.5 $cm^2$) was cleaned with 3 M HCl to remove any surface oxides and then washed with acetone, ethanol and deionised water for 30 min each, followed by overnight drying at 60 °C. 1 mg of NMC catalyst (pristine or recovered) was dispersed in Nafion (100 μL) and ethanol/water solvent in a 1 : 1 ratio followed by 60 min sonication. 300 μL of this ink was then used for immobilising the NMC material on the NF and dried at 60 °C overnight. For OER experiments the potential was converted to the RHE scale and the current density was normalised to the geometric surface area of the electrode. LSV curves were recorded with $iR_u$ compensation at 85%.

### Characterisation

The morphology of the samples was analysed by scanning electron microscopy (SEM) and energy dispersive spectroscopy (EDS) using a JEOL 7001F electron microscope. X-ray photoelectron spectroscopy (XPS) data was collected using an Omicron Multiclan Lab Ultra-High Vacuum Scanning Tunnelling Microscope (UHV-STM).

## Results and discussion

Previous comparative studies between different types of NMC battery cathode materials such as NMC 811 and NMC 622 indicated that NMC 622 was a superior electrocatalyst for the OER.[12] However, the impact of battery cycling was not explored and how that may influence the OER activity of the recovered material. Therefore, the OER behaviour of unused NMC 622 as well as cycled NMC 622 recovered from Li ion batteries, was examined in detail for their OER performance.

The batteries used to source the cycled NMC 622 were subjected to 8 formation cycles with discharge rates of 3 × C/10 and 5 × C/5, combined with the same charge rates. The formation cycles were followed by a rate test (1 × C/10, C/5, C/2, 1C, 2C, 3C) to deliberately induce stress and accelerated ageing effects. Finally, an arbitrary number of cycles at 1C were performed,

Table 1 Cell components and performance summary[a]

| Cell ID | Cathode ML NCM622 (mg $cm^{-2}$) | Anode ML graphite (mg $cm^{-2}$) | Neg./pos. ratio | Life cycle count @1C | Theoretical capacity (mAh) | Cycle 7: C/10 discharge capacity (mAh) |
|---|---|---|---|---|---|---|
| Cell 1 | 12.64 | 7.55 | 1.34 | 50 | 52.05 | 50.79 |
| Cell 2 | 12.62 | 7.33 | 1.30 | 150 | 51.97 | 50.63 |
| Cell 3 | 12.73 | 7.39 | 1.30 | 200 | 52.42 | 49.09 |

[a] Electrolyte contained in all cells was LP40 in 1 : 1 EC/DMC (1.3 g).

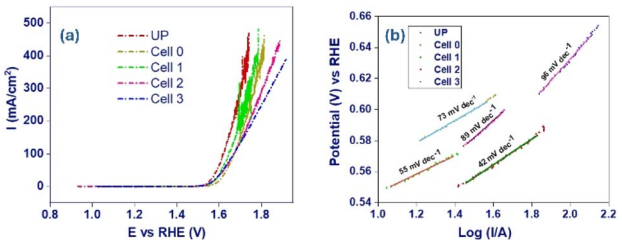


Fig. 1 (a) LSVs recorded at 0.1 mV $s^{-1}$ between 1.0 to 1.9 V in 1 M KOH and (b) corresponding Tafel plots.

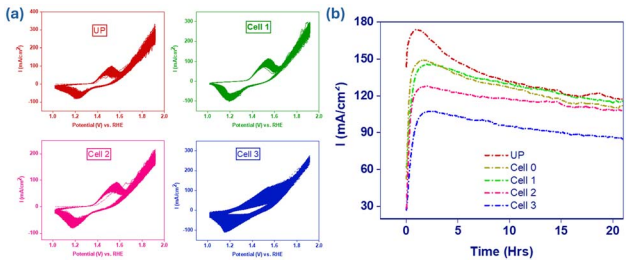


Fig. 2 (a) Cyclic voltammograms recorded at 100 mV $s^{-1}$ for 2000 cycles and (b) chronoamperometric experiments conducted at 1.7 V for 21 h for UP, Cell 0, Cell 1, Cell 2 and Cell 3 electrodes in 1 M KOH.

with the number of cycles varied from 50 to 200 depending on the sample identifier (Table 1). All charging cycles after formation were completed with a C/2 charge current.

The OER activity in Fig. 1a is shown by slow scan rate (0.1 mV $s^{-1}$), linear sweep voltammetry (LSV) from 1.0 to 1.9 V *vs.* RHE in 1 M KOH. The unprocessed sample (UP) was not assembled into a battery and shows the earliest onset potential (1.54 V) and highest current density in the potential region of study. The next sample of NMC 622 was assembled in a battery but not cycled (Cell 0). When the sample denoted Cell 0 was recovered from the battery and tested, it showed decreased performance. This is reflected by a later onset potential (1.58 V) and lower current density for Cell 0 (Fig. 1a). Therefore, the process of pouch cell assembly and subsequent disassembly for the recovery of NMC 622 from the binder, impacts slightly on performance. Interestingly after 50 battery cycles (Cell 1) the material showed some recovery in its OER performance with an onset potential of 1.56 V and improved current density. This may be due to some structural or surface compositional changes of the material during lithiation/de-lithiation that introduces sites that may be more active for the OER. Upon further battery cycling for 150 cycles (Cell 2) and 200 cycles (Cell 3) the onset potential remained constant, however the current density decreased indicating that battery cycling has an impact on OER activity. It should be noted that the same mass of active material is used for all electrodes.

Promisingly, all the electrodes achieve substantially high current densities of up to 400 mA $cm^{-2}$ in the potential window of study indicating practical applicability. The potential required to reach a current density of 100 mA $cm^{-2}$ was 1.62 V for UP, 1.64 V for Cell 1 and 1.67 V for Cell 2, Cell 3, and Cell 0. The Tafel slopes were then determined as shown in Fig. 1b where values of 42, 55, 73, 89 and 96 mV $dec^{-1}$ were calculated for electrodes UP, Cell 1, Cell 0, Cell 2, and Cell 3, respectively. This trend shows a gradual reduction in electron transfer kinetics with increased cycles of the material in a battery. The durability and stability of the electrodes were evaluated by subjecting them to 2000 potential cycles between 1.0 and 1.9 V at a sweep rate of 100 mV $s^{-1}$, as illustrated in Fig. 2a. During repeated cycling, the magnitude of the oxidation process at *ca.* 1.5 V increased and shifted to higher potentials indicating potential changes in the electrode's surface area and modifications in its surface composition with possible formation of metal oxides phases and introduction of metal hydroxide species on the surface after cycling. Even though the redox process prior to the OER increased with cycling, the OER activity is observed to decrease in all cases. This may be related to the low conductivity of transition metal oxide/hydroxide species which would negatively impact OER performance when thicker films are created during repetitive potential cycling. It was found that the final current density being passed after 2000 cycles is lowest for Cell 3 which indicates that battery cycling impacts long term durability under these accelerated ageing conditions. The electrodes were then tested under continuous electrolysis conditions and held at 1.7 V for 21 h (Fig. 2b). As expected, a similar trend is observed to the cyclic voltammetric data in Fig. 1a. After *ca.* 2 h of electrolysis there is a peak in performance of all electrodes and after 21 h of electrolysis the current densities were all within 10% of each other except for Cell 3 which showed significantly reduced current density indicating that more extensive battery cycling is detrimental to OER performance.

The electrochemical analysis of the NMC materials presents interesting observations that lead to the conclusion that more extensive battery cycling of up to 200 cycles leads to worse performance for the NMC 622 electrodes. It has been reported in a previous study that when $LiCoO_2$ is cycled more extensively in a battery, that more active sites become available and the OER improves.[11] However it should be noted that NMC 622 is a significantly different material to $LiCoO_2$ while there are also differences between the charge/discharge rates used and the loading of active material compared to binder and carbon in the two studies. Therefore, direct comparison of activity differences due to cycling are difficult to make given such different experimental arrangements.

To understand this outcome the NMC 622 pristine powder of sample UP and recovered from Cell 3 (200 cycles) were observed by SEM prior to any OER experiments to understand the surface morphology changes that may arise due to battery cycling. As shown in Fig. 3a, SEM images of the UP sample show that the particles are well distributed with sizes in the order of microns (Fig. 3b) that are in close proximity but not agglomerated. Upon closer inspection each larger particle consists of smaller particles that are less than 1 micron in diameter (Fig. 3c). However, the structures of NMC 622 recovered from Cell 3 shown in Fig. 3d are distinctly different with much smaller particles that

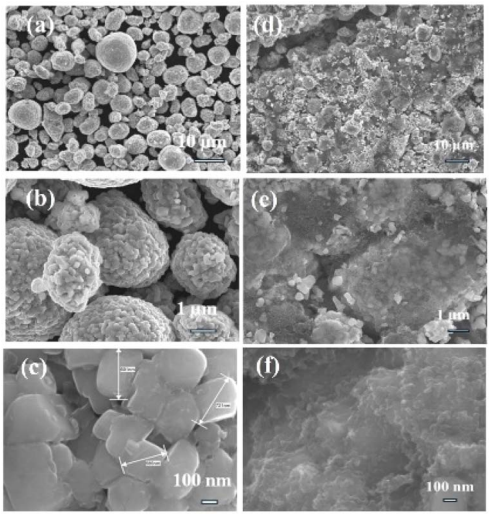


Fig. 3 SEM images of (a–c) unprocessed UP (NMC-622) sample and (d–f) NMC 622 recovered from Cell 3.

result in more film like formation on the substrate that contain large and deep cracks at the micro scale.

After cycling in the battery, the larger micron sized particles are reduced in size to the nanoscale that agglomerate across the electrode surface (Fig. 3e and f). The electrochemical surface area (ECSA) was determined *via* double layer charging experiments (Fig. 4) where the ECSA for the UP cell was 1.4 $cm^2$ and the Cell 3 sample was 1.67 $cm^2$. This indicates that the inherent specific activity of the recovered Cell 3 material is significantly lower due to battery cycling even the though the surface area was higher due to particle pulverisation. After repetitive cycling in the OER region, the ECSA for the UP sample increased to 1.85 $cm^2$ and 1.83 $cm^2$ for the UP and Cell 3 samples, respectively indicating that the specific activity of the recovered battery material is still lower.

Further studies were conducted to observe the oxidation states of the unprocessed sample (UP (NMC 622)) compared with NMC 622 recovered from Cell 3. It is observed in Fig. 5 that the Ni 2p core level spectrum shows peaks around 855.4 eV that belongs to Ni $2p_{3/2}$ for the $Ni^{2+}$ oxidation state with a satellite peak around 860.4 eV.[13] Peaks at 872.4,[14] 874.1 (ref. 15) and 878.4 eV belong to the Ni $2p_{1/2}$ orbital for the $Ni^{2+}$ oxidation state[16] that is attributed to the formation of hydroxides. Similar peaks were observed for NMC 622 from Cell 3. The high resolution XPS Co 2p spectrum for the UP (NMC 622) sample shows

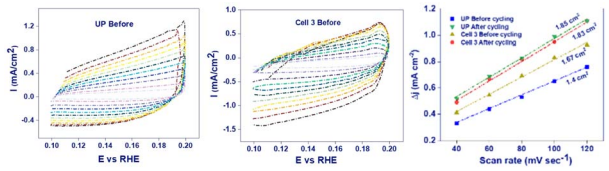


Fig. 4 CVs recorded from 40 to 120 mV $s^{-1}$ in 1 M KOH at UP (NMC-622) and NMC 622 recovered from Cell 3. Also shown are plots determining the ECSA for UP and Cell 3 before the OER and after being subjected to 2000 cycles in the OER region (1 to 1.9 V).

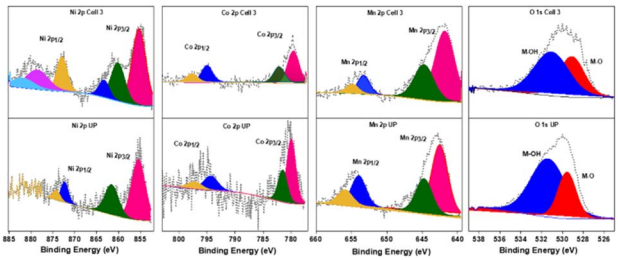


Fig. 5 XPS spectra for Ni 2p, Co 2p, Mn 2p and O 1s for UP (NMC 622) and Cell 3 recovered NMC 622.

peaks at 780.01 and 781.8 eV attributed to Co $2p_{3/2}$,[17,18] while the peak at 793.1 and 798.3 eV belongs to Co $2p_{1/2}$ representing the $Co^{2+}$ oxidation state.[19–21] For NMC 622 recovered from Cell 3 the XPS spectrum is mostly unchanged apart from a shift to a lower binding energy position from 780.0 eV to 779.6 eV indicating a more reduced Co surface species.

The high-resolution Mn 2p spectrum of NMC 622 (UP) shows prominent peaks at 642.5 and 653.6 eV that refers to $2p_{3/2}$ orbitals. Additionally, peaks at 644.7 eV and 656.1 eV belongs to Mn $2p_{1/2}$ for the $Mn^{2+}$ oxidation state.[16,22] For NMC 622 from Cell 3 a similar set of peaks were observed, however there is also a slight decrease in binding energy for the main peak to 642.1 eV as seen for the case of Co 2p. Finally, the O 1s spectra for NMC 622 (UP) shows the prominent presence of hydroxyl groups in the form of M–OH and metal oxides (M–O). However, for NMC 622 recovered from Cell 3 the extent of M–OH groups on the surface is diminished. The XPS data indicates that there are minor differences in the surface chemistry of the particles for the unprocessed NMC 622 and the material recovered from a battery that was cycled 200 times. The differences are the lower amount of M–OH species and less oxidised Co and Mn species on the surface of the NMC 622 material after 200 battery cycles which may impact on the activity and stability of the electrode. This result indicates that this proposed direct recycling approach is most suited to NMC 622 containing LIBs that fail quality assurance tests after their production. This may be a viable economic pathway to recover the cost incurred for failed cells that still undergo the formation and aging steps during their manufacture which account for approximately one-third of the manufacturing cost allocation.

## Conclusions

This study contributes important missing information for the potential use of recovered NMC 622 battery materials as OER electrocatalysts. It was found that battery history impacted the electrocatalytic activity of the recovered material where increasing the number of battery cycles resulted in a gradual decrease in performance for the OER. The particles recovered from an NMC 622 battery that was cycled 200 times had a significantly changed morphology with higher surface area than the pristine NMC 622 with a slightly more reduced surface chemistry containing fewer M–OH species. This resulted in the inherent specific activity of the recovered material being lower

for the OER. This outcome however opens a pathway for the often-overlooked problem of battery scrap that is produced during battery manufacturing consisting of cells that fail quality assurance tests. Recycling these NMC 622 cathodes may be a viable route to recover the costs associated with manufacturing such failed cells.

## Author contributions

Arshdeep Kaur: conceptualisation; data curation; methodology; writing – original draft. Hongxia Wang: supervision; writing – review & editing. Michael Horn: investigation; methodology; writing – review & editing. Jessica Crawford: data curation; methodology; writing – review & editing. Anthony O'Mullane: conceptualisation; methodology; resources; supervision; writing – review & editing.

## Conflicts of interest

There are no conflicts to declare.

## Data availability

Data for this article, including [electrochemical, XPS, SEM] are available at Open Science Framework at **https://www.osf.io/z89vy**.

## Acknowledgements

AOM acknowledges partial funding from the Australian Research Council (DP180102869, IH190100009). The authors acknowledge the instrumentation and technical support of the QUT Central Analytical Research Facility (CARF) and scholarship support through the QUT/Max Planck Institute of Colloids and Interfaces Joint Laboratory on Nanocatalysis for Sustainable Chemistry. MRH and JC acknowledge funding support from the Electrochemical Testing Project (Project 022) of the Future Battery Industries Cooperative Research Centre.

## Notes and references

1 Q. Jiang, N. Chen, D. Liu, S. Wang and H. Zhang, *Nanoscale*, 2016, **8**, 11234.
2 Y. Chu, Y. Mu, L. Zou, F. Wu, L. Yang, Y. Feng and L. Zeng, *ChemElectroChem*, 2024, **11**, 00653.
3 W. M. Dose, W. Li, I. Temprano, C. A. O'Keefe, B. L. Mehdi, M. F. L. De Volder and C. P. Grey, *ACS Energy Lett.*, 2022, **7**, 3524.
4 Q. Wei, Y. Wu, S. Li, R. Chen, J. Ding and C. Zhang, *Sci. Total Environ.*, 2023, **866**, 161380.
5 D. Latini, M. Vaccari, M. Lagnoni, M. Orefice, F. Mathieux, J. Huisman, L. Tognotti and A. Bertei, *J. Power Sources*, 2022, **546**, 231979.
6 L. Yu, Y. Bai, B. Polzin and I. Belharouak, *J. Power Sources*, 2024, **593**, 233955.
7 J. Fleischmann, M. Hanicke, E. Horetsky, D. Ibrahim and M. van de Rijt Linder, *Battery 2030: Resilient, Sustainable, and Circular*, McKinsey & Company Report, 2023.
8 S. Castillo, *J. Power Sources*, 2002, **112**, 247.
9 J. Xu, H. R. Thomas, R. W. Francis, K. R. Lum, J. Wang and B. Liang, *J. Power Sources*, 2008, **177**, 512.
10 H. Saleem, M. Khosravi, S. Maroufi, V. Sahajwalla and A. P. O'Mullane, *Sustainable Energy Fuels*, 2022, **6**, 4829.
11 N. Chen, J. Qi, X. Du, Y. Wang, W. Zhang, Y. Wang, Y. Lu and S. Wang, *RSC Adv.*, 2016, **6**, 103541–103545.
12 A. Kaur, J. Alarco and A. P. O'Mullane, *ChemPhysChem*, 2024, **25**, e202400124.
13 U. K. Sultana, J. F. S. Fernando and A. P. O'Mullane, *Sustainable Mater. Technol.*, 2020, **25**, e00177.
14 P. Babar, A. Lokhande, V. Karade, B. Pawar, M. G. Gang, S. Pawar and J. H. Kim, *J. Colloid Interface Sci.*, 2019, **537**, 43.
15 A. Sivanantham, P. Ganesan and S. Shanmugam, *Adv. Funct. Mater.*, 2016, **26**, 4661.
16 K. E. Salem, A. A. Saleh, G. E. Khedr, B. S Shaheen and N. K. Allam, *Energy Environ. Mater.*, 2022, **6**, e12324.
17 R. Arian and A. M. Zardkhoshoui, *ChemElectroChem*, 2020, **7**, 2816.
18 D. Chinnadurai, R. Rajendiran, O. L. Li and K. Prabakar, *Appl. Catal., B*, 2021, **292**, 120202.
19 H. Cao, Y. Xie, H. Wang, F. Xiao, A. Wu, L. Li, Z. Xu, N. Xiong and K. Pan, *Electrochim. Acta*, 2018, **259**, 830.
20 U. K. Sultana, J. D. Riches and A. P. O'Mullane, *Adv. Funct. Mater.*, 2018, **28**, 1804361.
21 B. Lu, J. Zang, W. Li, J. Li, Q. Zou, Y. Zhou and Y. Wang, *Chem. Eng. J.*, 2021, **422**, 130062.
22 P. P. Dhakal, U. N. Pan, D. R. Paudel, M. R. Kandel, N. H. Kim and J. H. Lee, *Mater. Today Nano*, 2022, **20**, 100272.